Sensors and Materials, Vol. 37, No. 3 (2025) 1259–1270
MYU Tokyo

S & M 3985

Real-time Motor Fault Detection System Using Microcontroller

Teh-Lu Liao,[1] Jun-Juh Yan,[2] and Chih-Yung Chen[1,3*]

[1]Department of Engineering Science, National Cheng Kung University,
No. 1, University Road, Tainan City 701, Taiwan (R.O.C.)
[2]Department of Electronic Engineering, National Chin-Yi University of Technology,
No. 57, Sec. 2, Zhongshan Road, Taiping District, Taichung 411030, Taiwan (R.O.C.)
[3]Bachelor Program in Artificial Intelligence and Mechatronics, National Pingtung University of Science and Technology, No. 1, Shuefu Road, Neipu, Pingtung 912, Taiwan (R.O.C.)

(Received June 30, 2024; accepted March 14, 2025)

Keywords: motor fault detection, discrete wavelet transformation, microcontroller, vibration, self-organizing map, accelerometer

In this study, we present an integrated motor inspection system utilizing digital processing techniques, which can be applied in fields such as factory automation, electric vehicles, and mechanical arms. The system collects signals from multiple sensors placed around the motor and triggers specific alarm signals upon detecting fault conditions. In the proposed approach, a microcontroller is used to monitor the motor operation continuously. Initially, it receives temperature signals from an infrared sensor to assess whether the motor temperature falls within the specified working range. Additionally, current and noise sensors are utilized to measure whether the current and noise levels exceed the respective rated limits. Furthermore, a Hall magnetic rotation position sensor determines the speed and motor rotation angles, enabling the detection of issues related to speed and current. Moreover, a three-axis accelerometer installed on the motor gauges motor vibrations. Subsequently, the discrete wavelet transformation is applied to segregate vibration signals into the domains, enabling the identification of abnormal vibrations resulting from electrical or mechanical issues using statistical methods. Finally, the system can transmit inspection results to an external panel via serial communication for graphical display. The proposed system can effectively detect motor faults and ensure the motor's normal operation. It is designed to facilitate real-time monitoring and aid maintenance personnel in troubleshooting.

1. Introduction

Motors are crucial in various fields, including industrial manufacturing, transportation, and household appliances. However, traditional motor inspection methods have several limitations and challenges, such as disassembly, monitoring, and measurement difficulties. These intermittent inspection methods may fail to detect potential motor issues or faults in time, leading to production interruptions, safety concerns, and increased maintenance costs. Common

*Corresponding author: e-mail: mikechen@mail.npust.edu.tw
https://doi.org/10.18494/SAM5226

ISSN 0914-4935

motor faults include overheating, insulation damage, bearing failures, power fluctuations, magnetic coil or brush issues, and mechanical structure damage or wear.(1,2) When performing maintenance, technicians must determine problems on the basis of the motor's specifications and abnormal conditions. General criteria for diagnosis include the following:

(1) **Vibration**: Understanding vibration is essential for assessing motor health. It can signal electrical or mechanical issues.(3–5) Built-in vibration sensors are costly, and adding them along with analyzing data can be pricey. Additionally, algorithms related to vibration diagnostics and the hardware required for these algorithms are relatively expensive and complex. However, vibration diagnostics are critical for ensuring motor operation.

(2) **Sound**: Unusual noises during motor operation often indicate problems with the motor, bearings, gears, or mechanical structures. This type of research emphasizes the filtering, transformation, and analysis of sound signals. Verifying motor fault diagnosis under various background conditions and with different microphones is a major focus of such research.(6)

(3) **Speed**: Abnormally high, low, or irregular speeds may suggest issues with the electrodes, coils, controllers, or other components of motors. Additionally, issues such as bearing faults, shaft misalignment, and rotor unbalance can also be identified through further analysis of rotational signals.(7)

(4) **Temperature**: The motor's operating temperature should remain within a normal range. Excessive temperatures can indicate overloading, cooling system failures, or other issues, which are usually associated with multiple causes. This is not only a matter of fault detection but also an important area of research for safety precautions.(8)

(5) **Current**: Voltage or current levels exceeding specifications could signal power supply issues or potential problems with the motor's rotor or stator coils. The current detection methods employed are noninvasive, making them preferred in practical applications. The techniques involve analyzing specific motor current characteristics to identify and address any issues accurately.(9–12)

Therefore, in this research, we propose an integrated real-time monitoring system with these functionalities embedded in motor equipment, which can be applied to robotic arms, automotive power motors, and other applications. This system can promptly detect motor abnormalities, effectively reduce maintenance time and costs, and improve maintenance efficiency.

2. Multisensor Embedded System for Motor Inspection

As shown in Fig. 1, a motor inspection system was developed, employing a range of sensors, including vibration, current, temperature, and speed detectors. The system uses discrete wavelet transform (DWT) to convert the vibration sensor data into the frequency spectrum. Subsequently, all parameters are subjected to digital signal processing and statistical analysis to determine the operational status of the motor. This enables the system to detect abnormalities, predict faults, and estimate maintenance needs.

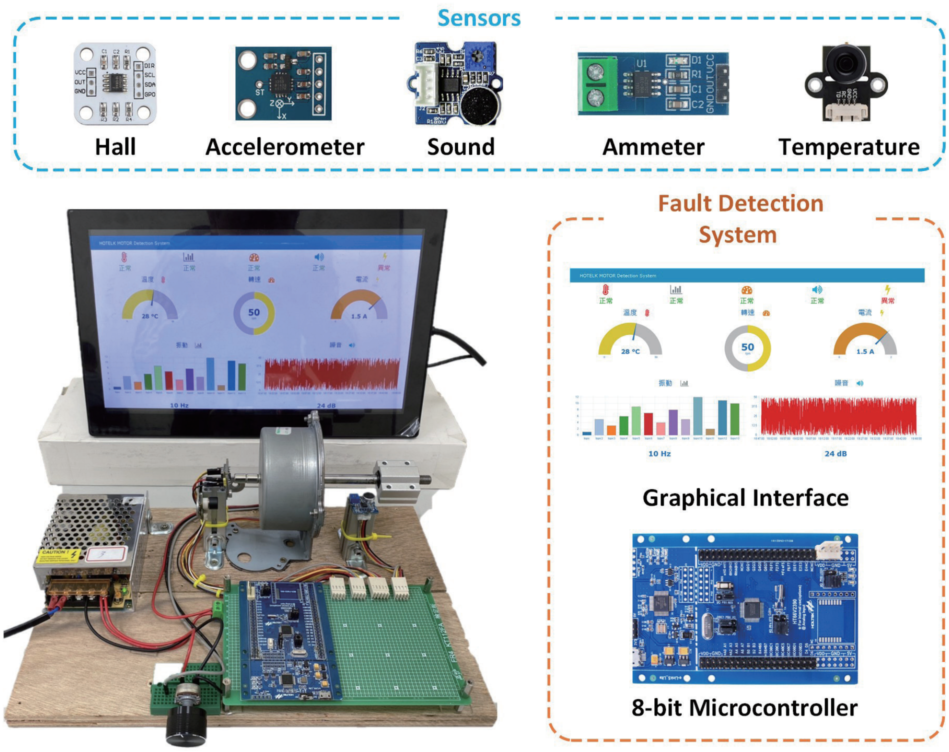

Fig. 1. (Color online) Proposed motor inspection system.

3. Real-time Vibration Signal Analysis Algorithm

Using vibration signals to analyze whether a motor is abnormal is a commonly used method in many studies.[3–5] Owing to the difficulty of time domain analysis, converting to frequency domain space, such as using the Fourier transform,[13] is the most common signal preprocessing method. However, setting up a signal processing system capable of performing Fourier transform might be prohibitively expensive for a typical motor, making it impractical for actual application. Therefore, the algorithm design in this study focuses on low computational cost, choosing lighter transformation methods and combining them with less computationally intensive decision-making methods to establish an economical motor fault detection system.

3.1 Lifting 5/3 DWT

In the proposed system, the motor's accelerometer can measure vibration signals, allowing the estimation of any abnormalities during operation. However, analyzing these continuous-time vibration signals can be challenging. To separate abnormal vibration and normal rotation signals, the proposed approach applies the DWT to develop filters for noise reduction.[14] DWT decomposes the signal into high-frequency coefficients (details) and low-frequency coefficients (approximation), as shown in Fig. 2.

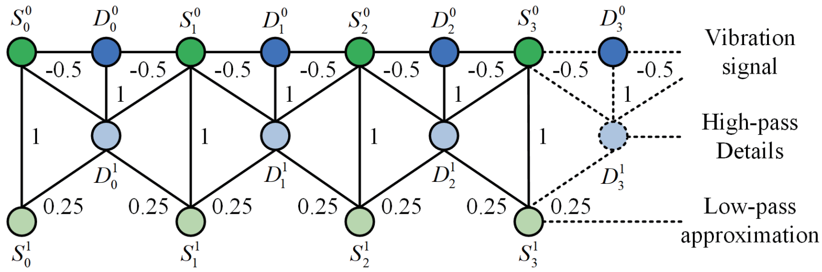

Fig. 2. (Color online) Lifting 5/3 DWT algorithm.

The DWT offers the advantage of computational simplicity, making it feasible for implementation even on platforms with low computational resources. In this study, we utilized the Lifting 5/3 method within the DWT for data reduction and signal extraction. The Lifting 5/3 method is known for its high computational efficiency and extremely low computational complexity. The computational process can be generally categorized into two steps:

1) Splitting step

   This step assumes that the vector variable $\boldsymbol{d}$ with m data points (for example, the input vibration values) can be divided into two parts: odd-numbered points and even-numbered points, which are represented by S and D, respectively. The calculation method is described as

$$S_i^0 = d_{2i+1},\ D_i^0 = d_{2i},\ \forall(d_{2i+1}, d_{2i}) \in \boldsymbol{d}, \text{ and } i = 0,1,2,...\frac{m}{2}. \tag{1}$$

2) Lifting step

   This step can separate out the high-frequency coefficients D_i^1 and the low-frequency coefficients S_i^1, which are represented as

$$D_i^1 = D_i^0 - \frac{(S_i^0 + S_{i+1}^0)}{2} \text{ and } S_i^1 = S_i^0 + \frac{(D_{i-1}^1 + D_i^1)}{4}. \tag{2}$$

DWT can be completed using the two simple steps mentioned above. The result of the computation after two repetitions of DWT is called the second-order wavelet transform. After the computation, the high-frequency signal will be reduced to only one-quarter of the original data size. Note that no significant feature reduction can effectively reduce the computation time of complex algorithms in the following calculations. In this study, the accelerometer captures a vibration value every 2 ms, and after gathering 128 data points, two wavelet transforms are performed. The 32 high-frequency components retained are used for subsequent computations.

3.2 Box plot and five-number summary

A box plot is a commonly used method for visualizing data that displays a five-number summary, namely, the minimum, first quartile, median, third quartile, and maximum. As shown in Fig. 3, the two ends of the box represent the first quartile Q_1 and third quartile Q_3 of the dataset. The vertical line inside the box represents the median of the dataset, and the values presented at the two endpoints represent the minimum and maximum values.

To enhance computational performance, we computed the five-number summary of the data processed by the previously mentioned DWT. This method utilizes only five data points to describe the high-frequency components of the vibration signals, which facilitates rapid and real-time classification to identify the presence of any anomalies.

3.3 Self-organizing map (SOM)

SOM is a type of unsupervised neural network. Its basic principle is to simulate the characteristics of the human brain, where brain cells with similar functions cluster together. This neural network is developed to learn data that exhibits clustering classification rules, making it suitable for SOM networks.(15) The structure of SOM is simple, as shown in Fig. 4. It consists of only one input layer and one output layer, also known as the Kohonen layer.

In SOM, the neurons in the output layer are arranged in a matrix in either 1D or 2D space. Each neuron is interconnected with other neurons to form a meaningful topological structure. The feature map refers to neurons competing to adjust connection weights based on the input vector.

Consider an input vector $\boldsymbol{x}$, which comprises motor revolutions per minute (rpm) and the five-number summary of vibration sensor data processed by DWT, and an output layer vector $\boldsymbol{k}$, which represents normal and abnormal categories.

$$\boldsymbol{x} = [x_1, x_2, ..., x_n]^T \quad \text{and} \quad \boldsymbol{k} = \begin{Bmatrix} k_{11} & \cdots & k_{1N} \\ \vdots & \ddots & \vdots \\ k_{N1} & \cdots & k_{NN} \end{Bmatrix} \tag{3}$$

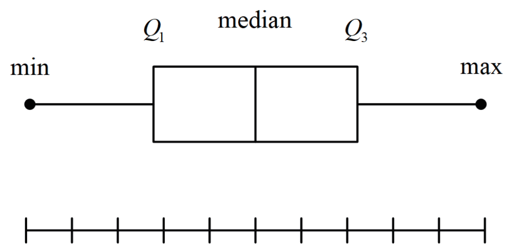

Fig. 3. Box plot and five-number summary.

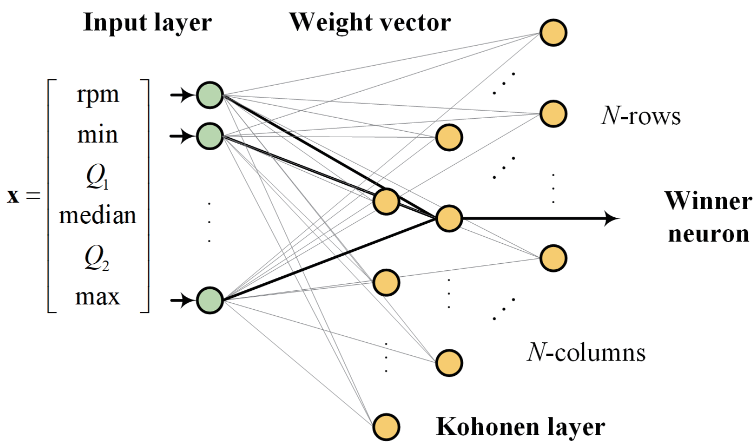

Fig. 4. (Color online) SOM structure.

Here, n is the quantity of input data $\boldsymbol{x}$, representing motor's rpm and the five-number summary (n = 6), and N is the number of rows and columns in the output layer.

Therefore, the weight vector $\boldsymbol{w}_{ij}^{k}$ connecting to the neurons k_{ij} in the output layer can be represented as

$$\boldsymbol{w}_{ij}^{k} = [w_{ij1}^{k}, w_{ij2}^{k}, \ldots, w_{ijn}^{k}]^{T}, \tag{4}$$

where i and j are the row and column indices, respectively, for the output neuron k.

When SOM begins learning, the connection weight vectors $\boldsymbol{w}_{ij}^{k}$ for the input vector $\boldsymbol{x}$, which are fully connected to the output layer $\boldsymbol{k}$, are assigned randomly. Assuming that the best-matching output neuron is represented as $b(\boldsymbol{x})$, it can be identified using the shortest Euclidean distance calculation, which is

$$b(\boldsymbol{x}) = \{(i, j),\ \arg\min_{i,j} \left\| \boldsymbol{x} - \boldsymbol{w}_{ij}^{k} \right\| \}. \tag{5}$$

Once a best-matching neuron is found, the weights of the winning neuron and its topologically neighboring neurons are also adjusted. The equations for the adjustment can be represented as

$$\boldsymbol{w}_{ij}^{k}(t_k + 1) = \boldsymbol{w}_{ij}^{k}(t_k) + \eta_k(t_k) h_{\boldsymbol{b}(\boldsymbol{x})}(t_k)(\boldsymbol{x} - \boldsymbol{w}_{ij}^{k}(t_k)), \tag{6}$$

$$h_{\boldsymbol{b}(\boldsymbol{x})}(t_k) = \exp\left(-\frac{\sqrt{([i, j] - b(\boldsymbol{x}))^2}}{2\sigma^2(t_k)}\right), \tag{7}$$

where t_k represents the current iteration index and $0 \le \eta_k(t_k) \le 1$ is the learning rate, which gradually decreases over the learning period. $h_{\boldsymbol{b}(\boldsymbol{x})}(t_k)$ is the formula for calculating the neighboring neurons centered on $b(\boldsymbol{x})$, and $\sigma(t_k)$ is the parameter for the width of the neighborhood range, which also gradually decreases over the learning period.

Repeat Eqs. (5) to (7) until the learning process is complete. The termination condition can be set to a fixed number of training iterations or when the learning results converge. Input the training data of abnormal vibrations occurring in motors under various speeds and loads into SOM, such as bearing anomalies, casing vibration abnormalities, insufficient lubrication, and coupling anomalies. After training, the weights of the output layer of SOM can be used for feature clustering and implemented on an 8-bit microcontroller. When the motor is in operation, the data returned by the accelerometer, after being filtered through DWT and processed by the five-number summary calculation, is input into the SOM classifier, and the system can immediately issue an alert signal. The training process may be complex, but once it is finished, there is no need to relearn during actual use. The decision-making of the proposed approach is very fast, making it highly suitable for applications where installing high-computing or high-priced processors is not feasible.

4. Experimental Results

An 8-bit microcontroller module with 12 MHz working frequency, 32 KB data memory, and 1 MB program memory was utilized in this study for all programming tasks. A DC motor was used as the test subject. Around the motor, an accelerometer, a sound sensor, a Hall effect sensor, a temperature sensor, and a current sensor were installed, as shown in Fig. 5. In accordance with Ref. 16, we utilized Node-RED, a programming language development tool, to create a data observation interface for motor inspection. This interface receives data from the microcontroller via serial communication. When the motor is in operation, the data from all sensors will be displayed on the graphical interface. In the case of a motor anomaly, the microcontroller will use calculations to detect the issue and then send the corresponding signal to be displayed on the screen.

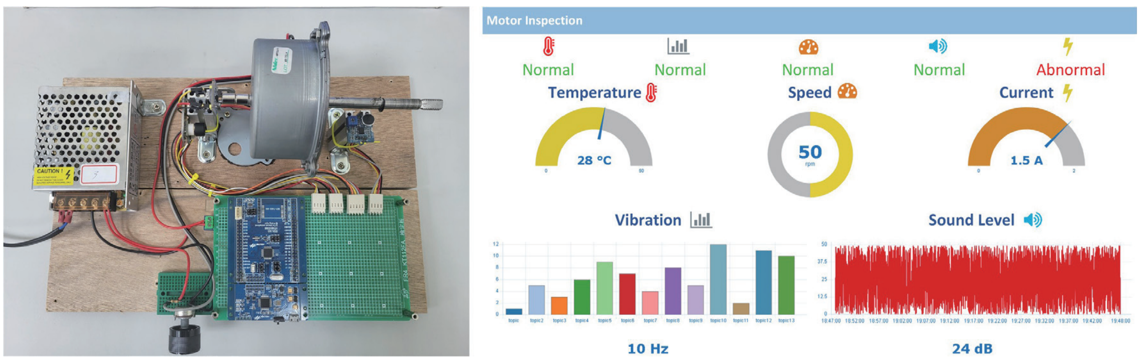

Fig. 5. (Color online) Installation motor inspection system and graphical interface.

4.1 Real-time multisensor measurement

Microcontroller polling and interrupt programming techniques were employed to develop high-speed sensor data acquisition functions in this study. Figure 6 shows the results of the experimental data capture for sound, rotational speed, temperature, and current. In this study, the determination method for these sensors depends on whether the sensor data exceeds or falls below the set threshold during the observation.

Figure 6(a) shows a digital microphone capturing sound signals. When the decibel level of the sound is below the set threshold, it will be determined as normal operation. The resulting loud noise will be considered an anomaly when the motor is connected to a damaged bearing.

Figure 6(b) shows the Hall sensor capturing the position of the motor rotor. Each complete waveform cycle represents one full rotor rotation, allowing for precise rotor position and motor speed calculation. Any deviation from this signal indicates the abnormal motor speed caused by external forces or other issues.

Figures 6(c) and 6(d) show the temperature and current sensors of the motor, respectively. When the motor operates outside the designated temperature or current range, such as when the motor casing generates unusually high temperatures or when the motor mechanism is subjected to abnormal forces causing unusual current flow, the system will issue an alarm in such cases.

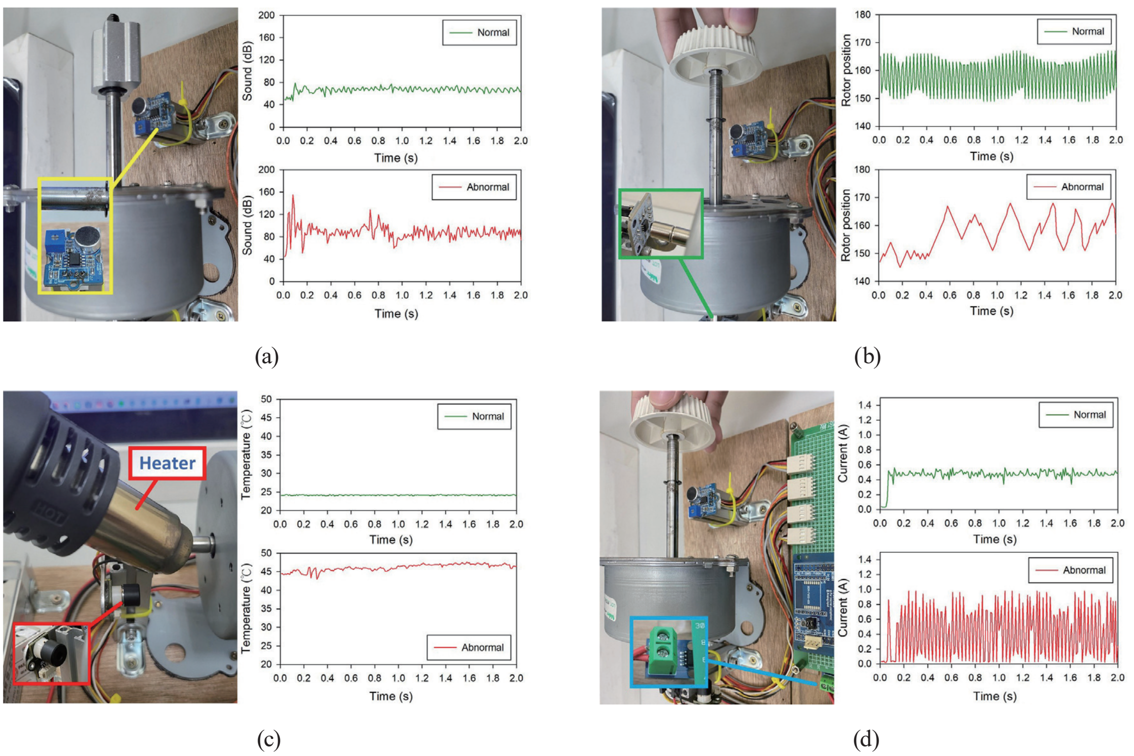

Fig. 6. (Color online) Multisensor signal measurement. (a) Sound sensor. (b) Hall effect sensor. (c) Temperature sensor. (d) Current sensor.

4.2 Vibration signal experimental results

Figure 7 illustrates the specific acceleration values that have been measured by an accelerometer while the motor was operating at 1800 rpm. During smooth motor operation, the acceleration values tend to remain within a lower range, specifically within ±1 g, as observed in our experiment. However, the presence of a defective and unbalanced bearing installed on the motor shaft can cause irregular vibrations, resulting in heightened variations that are detectable by the accelerometer. This increase in acceleration value serves as an indication of the abnormal behavior caused by the faulty bearing.

Since vibration signals can vary depending on the current, load, and speed conditions, using a fixed threshold for error detection is not feasible. In this study, we used DWT, five-number summary, and SOM methods to analyze signals. We collected a training dataset of 540 records, with 296 normal and 244 abnormal records for training, and a test dataset of 500 records, with 334 normal and 166 abnormal records, to validate the proposed method's effectiveness. The confusion matrix visualizes the results of both datasets, as shown on the right-hand side of Fig. 7.[17] The values 0 and 1 on the x- and y-axes represent normal and abnormal records, respectively.

The classification reports for the training and test datasets are presented in Tables 1 and 2, respectively, and briefly described as follows. Accuracy rate is defined as the ratio of the number of correctly predicted examples to the total number of examples. The training and test data accuracy rates are 97 and 91%, respectively, indicating a strong capability for detecting motor anomalies by this method. Additionally, the precision of abnormal predicted results (the ratio of the number of correct positive predictions to the total number of predicted positives) for both the training and testing data in this experiment is as high as 100%. Such results indicate that the signals diagnosed as motor anomalies are indeed abnormal. This meets the requirements of practical scenarios and can provide maintenance personnel with stable and accurate repair recommendations.

In the experiment, the recall rate for the test dataset, representing the ratio of actual positive cases correctly identified, is 72%. Although the recall result may not be optimal, note that achieving such performance on a resource-constrained microcontroller platform using a variety

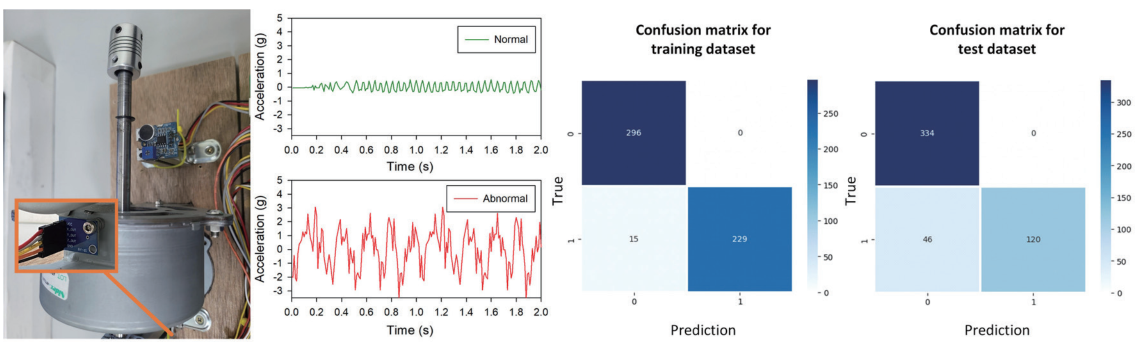

Fig. 7. (Color online) Vibration signal detection and confusion matrix analysis.

Table 1
Classification report for the training dataset.

	Precision	Recall	$F1$-score	Support
0 (Normal)	0.95	1.00	0.98	296
1 (Abnormal)	1.00	0.94	0.97	244
Accuracy			0.97	540
Macro avg	0.98	0.97	0.97	540
Weighted avg	0.97	0.97	0.97	540

Table 2
Classification report for the test dataset.

	Precision	Recall	$F1$-score	Support
0 (Normal)	0.88	1.00	0.94	334
1 (Abnormal)	1.00	0.72	0.84	166
Accuracy			0.91	500
Macro avg	0.94	0.86	0.89	500
Weighted avg	0.92	0.91	0.9	500

of algorithms for real-time diagnostics is noteworthy. It is necessary to pay attention to future improvements.

5. Conclusions

In this study, we implemented a low-computation-cost embedded motor inspection system that uses an 8-bit microcontroller to perform real-time detection from multiple sensors. Furthermore, DWT, five-number summary, and a SOM model are embedded into the microcontroller to classify normal and abnormal motor operation signals. This system also implements a visual graphical interface to display real-time data and alarm messages via serial communication from the microcontroller on a monitoring screen.

Experimental results showed that although the proposed algorithm is simple, it can detect abnormal motor signals quickly and efficiently. The accuracy of the test results can reach up to 91%, which is very effective for a microcontroller system with limited resources. Therefore, this system is highly suitable for extensive deployment in fields that use many motors. It provides a cost-effective way to monitor motor operations in real time, reducing the workload of maintenance personnel and preventing operational losses or hazards caused by malfunctions. As the system's recall performance needs improvement, algorithmic adjustments are necessary to enhance its value in future studies while preserving low complexity and efficiency.

Acknowledgments

This work was supported by the National Science and Technology Council under Grant nos. NSTC 111-2622-E-020-007 and NSTC 113-2637-E-020-002.

References

1 X. Liang, M. Z. Ali, and H. Zhang: IEEE Trans. Ind. Appl. **56** (2020) 1205. https://doi.org/10.1109/TIA.2019.2958908
2 S. Karmakar, S. Chattopadhyay, M. Mitra, and S. Sengupta: Induction Motor Fault Diagnosis: Approach Through Current Signature Analysis (Springer, Singapore, 2016).
3 M. Cerrada, R. Sánchez, C. Li, F. Pacheco, D. Cabrera, J. V. Oliveira, and R. E. Vásquez: Mech. Syst. Signal Process. **99** (2018) 169. https://doi.org/10.1016/j.ymssp.2017.06.012
4 M. Z. Ali, M. N. S. K. Shabbir, X. Liang, Y. Zhang, and T. Hu: IEEE Trans. Ind. Appl. **55** (2019) 2378. https://doi.org/10.1109/TIA.2019.2895797
5 H. Tang, S. Lu, G. Qian, J. Ding, Y. Liu, and Q. Wang: IEEE Sens. J. **21** (2021) 1820. https://doi.org/10.1109/JSEN.2020.3017768
6 T. Mian, A. Choudhary, and S. Fatima: Appl. Acoust. **195** (2022) 108839. https://doi.org/10.1016/j.apacoust.2022.108839
7 W. Jung, S. H. Kim, S. H. Yun, J. Bae, and Y. H. Park: Data Brief **48** (2023) 109049. https://doi.org/10.1016/j.dib.2023.109049
8 J. Pelegrin, U. J. Dreyer, J. P. Bazzo, and J. C. C. da Silva: IEEE Sens. J. **21** (2021) 20061. https://doi.org/10.1109/JSEN.2021.3097940
9 A. Allal and A. Khechekhouche: Int. J. Electr. Power Energy Syst. **141** (2022) 108219. https://doi.org/10.1016/j.ijepes.2022.108219
10 A. Sapena-Bano, F. Chinesta, M. Pineda-Sanchez, J. V. Aguado, D. Borzacchiello, and R. Puche-Panadero: Int. J. Electr. Power Energy Syst. **111** (2019) 315. https://doi.org/10.1016/j.ijepes.2019.03.020
11 T. A. Shifat and J. W. Hur: IEEE Access **8** (2020) 106968. https://doi.org/10.1109/ACCESS.2020.3000856
12 J. Chen, N. Hu, L. Zhang, L. Chen, B. Wang, and Y. Zhou: Appl. Sci. **10** (2020) 17. https://doi.org/10.3390/app10175980
13 Y. Xie, P. Chen, F. Li, and H. Liu: Mech. Syst. Signal Process. **123** (2019) 5980. https://doi.org/10.1016/j.ymssp.2019.01.030
14 R. A. Naseer, M. Nasim, M. Sohaib, C. J. Younis, A. Mehmood, M. Alam, and Y. Massoud: Integration **87** (2022) 253. https://doi.org/10.1016/j.vlsi.2022.07.009
15 T. Kohonen: Neural Networks **37** (2013) 52. https://doi.org/10.1016/j.neunet.2012.09.018
16 L. E. González-Jiménez, F. J. Arriaga-Méndez, O. F. Mendiola-Meza, and E. Vargas-Mascorro: IEEE Lat. Am. Trans. **19** (2021) 107. https://doi.org/10.1109/TLA.2021.9423853
17 D. Krstinić, L. Šerić, and I. Slapničar: IEEE Access **11** (2023) 40692. https://doi.org/10.1109/ACCESS.2023.3267672

About the Authors

Teh-Lu Liao received his B.S. degree (Hons.) from the Department of Engineering Science, National Cheng Kung University (NCKU), Taiwan, in 1982 and his M.S. and Ph.D. degrees (Hons.) from the Department of Electrical Engineering, National Taiwan University, Taiwan, in 1984 and 1991, respectively. He joined the Department of Engineering Science, NCKU, as an associate professor in 1991 and was promoted to full professor in 1999. His research interests include control theory, multi-agent systems, signal and image processing, chaos communication systems, and cryptosystems. (tlliao@mail.ncku.edu.tw)

Jun-Juh Yan received his M.S. degree in electrical engineering from National Central University, Taiwan, in 1992 and his B.S. and Ph.D. degrees in electrical engineering from National Cheng Kung University, Taiwan, in 1987 and 1998, respectively. At present, he is a professor in the Department of Electronic Engineering, National Chin-Yi University of Technology, Taichung, Taiwan. His main research interests are in the areas of multi-robot dynamic systems, chaotic systems, neural networks, variable-structure control systems, and adaptive control. (jjyan@ncut.edu.tw)

Chih-Yung Chen is an associate professor of the Bachelor Program in Artificial Intelligence and Mechatronics at National Pingtung University of Science and Technology, Taiwan. He received his B.S. and M.S. degrees in computer science and information engineering from Tamkang University in 1998 and 2000, respectively, and his Ph.D. degree in electrical engineering from I-Shou University in 2008. He is currently pursuing his second Ph.D. degree in the Department of Engineering Science at National Cheng Kung University in Taiwan. His research interests include artificial intelligence, database systems, and software engineering. (mikechen@mail.npust.edu.tw)